

Simultaneous forward- and backward-hemisphere elastic-light-scattering patterns of respirable-size aerosols

Gustavo E. Fernandes, Yong-Le Pan, and Richard K. Chang

Department of Applied Physics and Center for Laser Diagnostics, Yale University, New Haven, Connecticut 06520-8284

Kevin Aptowicz

Department of Physics, West Chester University, West Chester, Pennsylvania 19383

Ronald G. Pinnick

U.S. Army Research Laboratory, Adelphi, Maryland 20783

Received June 15, 2006; accepted July 18, 2006;
posted July 28, 2006 (Doc. ID 72013); published September 25, 2006

Two-dimensional angular optical scattering (TAOS) patterns of aerosols are measured simultaneously from the forward hemisphere $15^\circ < \theta < 90^\circ$ as well as the backward hemisphere $90^\circ < \theta < 165^\circ$ (detecting 63% of the 4π sr of scattered light) by using an ellipsoidal reflector and an intensified CCD detector. TAOS patterns were obtained from polystyrene-latex spheres (individuals and aggregates) and from single *Bacillus subtilis* spores. These information-rich patterns, measured with a single laser pulse for individual particles on the fly, suggest that forward-TAOS and backward-TAOS measurements may be used for rapid classification of single aerosol particles. © 2006 Optical Society of America

OCIS codes: 010.1100, 010.1110, 010.1310, 000.1430, 290.1310, 290.5850.

Airborne particles in the respiratory range (1–10 μm diameter) are important to fields ranging from climatology to human health.^{1–4} In recent years, two-dimensional angular optical scattering [TAOS, $I_s(\theta, \phi)$] has been investigated as a tool for the rapid characterization of biowarfare and other aerosols,^{5–8} because TAOS is sensitive to a particle's morphology and complex index of refraction. TAOS may provide information complementary to that extracted from other real-time aerosol measurement techniques, e.g., single-particle fluorescence,^{9,10} or laser-induced breakdown spectroscopy.¹¹

Recent experiments^{5–7} measured TAOS patterns of aerosols separately in either the forward hemisphere⁷ (F-TAOS) or the backward hemisphere^{5,6} (B-TAOS). In both cases an ellipsoidal reflector was employed to collect a large solid angle of scattered intensities for B-TAOS ($80^\circ < \theta < 168^\circ$ and $0^\circ < \phi < 360^\circ$) and for F-TAOS ($28^\circ < \theta < 141^\circ$ and $0^\circ < \phi < 360^\circ$). The F-TAOS measurements were performed on water droplets, salt crystals, polystyrene-latex (PSL) spheres, *Bacillus subtilis* (BG) spores and other particles with relatively simple geometries. The B-TAOS measurements were performed on fluid droplets (water, D₂O, and dioctyl phthalate), aggregates of PSL spheres, and aggregates of biological particles with several different geometries.^{5,6} The TAOS patterns obtained contained, in general, a large number of features (speckles and islands). Attempts were made in both the F-TAOS and the B-TAOS cases to extract information on the particle's geometry and refractive index from their scattering patterns. However, inversion results were in general inconclusive.

In this Letter we present, for the first time to our knowledge, TAOS results collected simultaneously in the forward and backward hemispheres (BF-TAOS). In a single measurement, by combining the scattering patterns in the forward and backward hemispheres, we have increased the θ angle range and decreased the ϕ angle range, whose information is redundant for spherical particles. At first glance it appears that there are more high-frequency features in B-TAOS than in F-TAOS. However, this is an artifact introduced by the detector noise associated with a weaker B-TAOS signal relative to the brighter F-TAOS signal.

For particles 1–10 μm in diameter, the resolution necessary to resolve the average feature size (i.e., distance between consecutive intensity peaks and valleys) present in the scattering pattern does not require the full intensified CCD (ICCD) resolution (1024 \times 1024 pixels). For example, two consecutive intensity maxima produced by a spherical 5 μm water droplet are separated by approximately 10° . For a single-hemisphere TAOS measurement^{5,6} the scattering pattern is collected over a range of approximately 90° in θ on a 1024 \times 1024 pixel detector. Each peak has a resolution of approximately 512/9, or 57 pixels. For two-hemisphere TAOS measurements, using a 512 \times 1024 pixel section for each hemisphere is sufficient to record changes as small as 3% (1/28.5) of the line shape of the main intensity peak.

We use the ellipsoidal reflector in a new configuration based on the illumination geometry shown in Fig. 1. The particles enter the reflector through the top hole and travel downward along the y axis. The scattering event occurs at the first focus (F1) of the

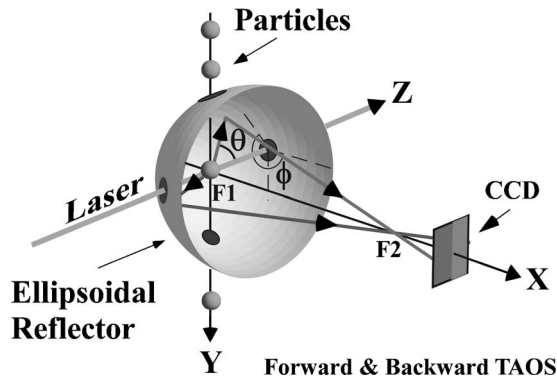


Fig. 1. Scheme for collecting the elastic-scattering intensity pattern in both forward and backward hemispheres simultaneously with an ellipsoidal reflector and CCD detector. The spherical coordinate angles θ and ϕ are defined with the laser beam propagating along the z direction and the symmetry axis of the reflector along the x direction.

ellipsoidal reflector. A large portion (63% of the 4π sr) of the light that is scattered by the particle is intercepted by the reflector and projected onto the ICCD detector. Half of the ICCD detects the backward-scattering pattern, and the other half detects the forward-scattering pattern. TAOS is measured for the azimuthal scattering angles in the range $15^\circ < \theta < 165^\circ$ and for polar angles covering as much as 360° in the near-forward and near-backward scattering and as little as 200° near the 90° meridian. The detector has five holes used for the passage of the laser beam, the triggering beams, and the particles.

For high-quality TAOS data, the particle position relative to the focal point F1 of the ellipsoidal reflector at the time of measurement is crucial. The intersection of two tightly focused cw TEM00 diode lasers (Microlaser Systems, with wavelengths at 635 and 685 nm) defines the trigger volume ($20\ \mu\text{m} \times 20\ \mu\text{m} \times 20\ \mu\text{m}$) centered at F1. When a particle passes through the intersection of both diode laser beams (and thus is in the trigger volume), the scattered light is detected by two photomultiplier tubes (each fitted with an interference filter at one of the diode laser wavelengths). The photomultiplier tube outputs need to exceed a threshold and be coincident before the AND circuit will issue a pulse to trigger the following: (1) the Nd:YAG laser (Spectra Physics, X-30) emits a 30 ns 532 nm pulse (second harmonic) to illuminate the particle; (2) the ICCD detector records the scattered intensity distribution; and (3) the two laser diodes used for triggering are pulsed off so that light from these lasers does not cause unwanted noise on the ICCD. Because the particles transit through F1 at speeds less than 5 m/s, the motion of the particle during the time of the laser pulse (30 ns) is less than $0.15\ \mu\text{m}$, which is much smaller than the particle size. We have assumed the particle to be stationary during the TAOS measurement. The aerosols were generated by an ink-jet aerosol generator (IJAG).¹²

The TAOS recorded in Cartesian coordinates Z_{ICCD} and Y_{ICCD} on the ICCD was transformed into TAOS in the particle coordinates θ and ϕ defined in Fig. 1. The

measured intensity $I(\theta, \phi)$ was plotted in two separate parts, corresponding to the forward $15^\circ < \theta < 90^\circ$ hemisphere and the backward $90^\circ < \theta < 165^\circ$ hemisphere, as shown in Fig. 2.

Figures 2(a)–2(d) show F-TAOS and B-TAOS patterns measured for clusters of $1.44\ \mu\text{m}$ diameter PSL spheres and Figs. 2(e)–2(h) for single BG spores. The mean number of PSL spheres per cluster was varied by varying the concentration of ink-jet-generated droplets (approximately $50\ \mu\text{m}$ in diameter) in the IJAG. Droplets with different PSL concentrations were prepared to provide different cluster sizes. Some representative samples were subsequently collected for observation with a scanning electron microscope. The mean number of particles per cluster for the samples in Figs. 2(a)–2(d) are 1 ± 0.7 , 2 ± 1.4 , 5 ± 2.2 , and 10 ± 3.2 particles.

Many TAOS patterns were measured for each cluster size. For each laser shot, the orientation of the particles relative to the laser-beam axis was random but was the same for a pair of B-TAOS and F-TAOS patterns. The pattern of Fig. 2(a) corresponds to a single PSL sphere. Concentric rings about the $\theta=0^\circ$ direction in the F-TAOS were more obvious than about the $\theta=180^\circ$ in the B-TAOS. The number and position of the intensity maxima between 0° and 75° correspond to those predicted by Mie theory.¹³

The elastic-scattering intensities in the forward hemisphere are much stronger than in the backward hemisphere. For a single ($1.44\ \mu\text{m}$) PSL sphere the

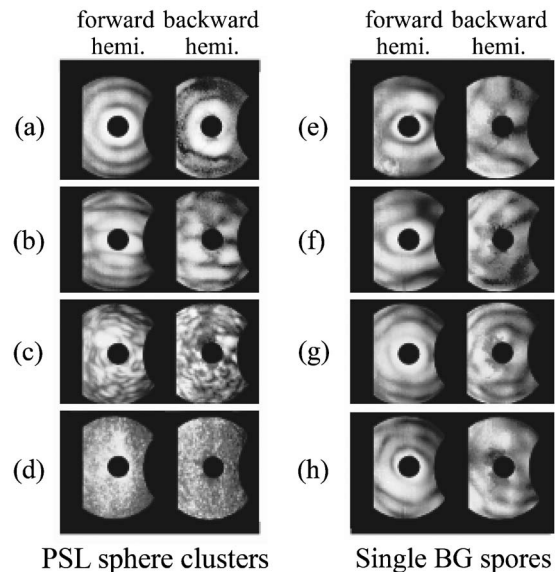


Fig. 2. Simultaneously recorded forward- and backward-hemisphere scattering patterns for clusters of (a)–(d) PSL spheres ($1.44\ \mu\text{m}$ in diameter) and (e)–(h) single BG spores. Each particle is illuminated by a single 30 ns laser pulse at $0.532\ \mu\text{m}$. The edge of the inner black circles in the forward and backward hemisphere patterns corresponds to $\theta=15^\circ$ and $\theta=165^\circ$, respectively. The outermost curved edge at the top and bottom of the patterns correspond to $\theta=90^\circ$. Each pattern was normalized separately so that their intensities would span the entire range of gray scales. For comparison, the peak intensities measured in the forward hemisphere were on average 80 times stronger than the backward hemisphere.

peak intensity detected in the forward hemisphere was approximately 80 times that in the backward hemisphere. This difference is well within the dynamic range of the ICCD detector used (approximately 1000). Attenuation of the forward half of the ICCD with a neutral-density filter was therefore not necessary. In displaying the recorded F-TAOS and B-TAOS in Fig. 2, the images for the forward and backward hemispheres were normalized separately so that their intensities would span the entire range of 256 gray scales from black (smallest value) to white¹⁴ (largest value).

The numbers of features (islands and speckles) for B-TAOS were compared with those in F-TAOS.¹⁵ The comparison, using MATLAB, consisted of the following steps: (i) the forward and backward hemisphere patterns were normalized independently so that their values would span the entire range of gray scales; (ii) a median filter with 5×5 pixels was applied to the images to reduce high-frequency background noise; (iii) the MATLAB function *imextended-max* was used to find the extended local maximums in the image; (iv) the images in step 3 were converted to binary images and the MATLAB routine *regionprops* was used to count the number of extended maximums present in each image. The procedure was applied to 100 images in the data sets corresponding to clusters of approximately 1–4 PSL spheres and for single BG spores. The average total number of counts (backward plus forward hemisphere counts) and the average backward-to-forward count ratio (average of the backward hemisphere counts divided by forward hemisphere counts) were computed, but it was found that the standard deviations in these averages were too high to enable us to draw any meaningful conclusion from them.

A few factors contribute to the large standard deviation in these numbers. First, because we are dealing with clusters of a small number of particles, the uncertainty in the number of particles per cluster is large [$\text{sqrt}(N)$, for a Poisson distribution, where N is the mean number of particles in the cluster]. Second, the cluster orientation relative to the laser beam changes, and that produces patterns with different distributions of islands in the forward and backward hemispheres. Furthermore, the procedure outlined above depends on setting a threshold for converting the gray-scale images into binary ones (blacks for valleys and whites for peaks) and has to rely on an educated guess before processing as to which features in the pattern correspond to islands.

In summary, we described a new configuration for simultaneously measuring the two-dimensional

angle-resolved elastic scattering from aerosol particles on the fly, in both the forward- and the backward-scattering hemispheres (BF-TAOS). BF-TAOS patterns for single and clusters of polystyrene latex spheres and single *B. subtilis* (BG) spores were measured. Analysis of the features in the BF-TAOS patterns was attempted through the use of an island counting routine, but results displayed a standard deviation too large to allow further conclusions to be drawn. We are currently working to improve the quality of our measurements by using a custom-made ellipsoidal reflector with a new design that is less prone to distortions.

We thank Steven C. Hill and Burt V. Bronk for their support and helpful discussions and Jerold R. Bottiger for providing use of the IJAG. We acknowledge the partial support from the U.S. Air Force Research Laboratory under contract F33615-02-6066. Gustavo E. Fernandes' email address is gustavo.fernandes@yale.edu.

References

1. D. A. Henderson, *Science* **283**, 1279 (1999).
2. P. J. Wyatt, *Nature* **221**, 1257 (1969).
3. L. A. Vanderberg, *Appl. Spectrosc.* **54**, 376a (2000).
4. T. Peter, *Science* **273**, 1352 (1996).
5. Y. L. Pan, K. Aptowicz, and R. K. Chang, *Opt. Lett.* **28**, 589 (2003).
6. K. B. Aptowicz, R. G. Pinnick, S. C. Hill, Y. L. Pan, and R. K. Chang, *J. Geophys. Res., [Atmos.]* **111**, D12212 (2006).
7. E. Hirst, P. H. Kaye, and J. R. Guppy, *Appl. Opt.* **33**, 7180 (1994).
8. E. Hirst and P. H. Kaye, *J. Geophys. Res., [Atmos.]* **101**, 19231 (1996).
9. R. G. Pinnick, S. C. Hill, P. Nachman, J. D. Pendleton, G. L. Fernandez, M. W. Mayo, and J. G. Bruno, *Aerosol Sci. Technol.* **23**, 653 (1995).
10. Y. L. Pan, S. Holler, R. K. Chang, S. C. Hill, R. G. Pinnick, S. Niles, and J. R. Bottiger, *Opt. Lett.* **24**, 116 (1999).
11. J. D. Hybl, G. A. Lithgow, and S. G. Buckley, *Appl. Spectrosc.* **57**, 1207 (2003).
12. J. R. Bottiger, P. J. Deluca, E. W. Stuebing, and D. R. Vanreenaen, *J. Aerosol Sci.* **29**, S965 (1998).
13. C. F. Bohren and D. R. Huffman, *Absorption and Scattering of Light by Small Particles* (Wiley, 1983).
14. The Andor iStar ICCD has a quantum efficiency of 10.75% at a wavelength of $0.532 \mu\text{m}$, and the minimum dark current achievable is 0.2 electron/pixel/s.
15. S. Holler, Y. L. Pan, J. R. Bottiger, S. C. Hill, D. B. Hillis, and R. K. Chang, *Opt. Lett.* **23**, 1489 (1998).